Oil Palm Bulletin 79 (November 2019) p. 9-15

Analysis of Red, Green, Blue (RGB) and Near Infrared (NIR) Images from Unmanned Aerial Vehicle (UAV) for Detection of *Ganoderma* Disease in Oil Palm

Izzuddin, M A*; Ezzati, B; Nisfariza, M N#; Idris, A S* and Alias, S A****

ABSTRACT

Ganoderma *disease in oil palm caused by* Ganoderma boninense *fungus has resulted in a significant loss of economic income to Malaysia. There is a need to develop an airborne-based* Ganoderma *disease detection technology to reduce cost and time, and to cover wide-scale oil palm plantation area. This study examines the performance of red-green-blue (RGB) and near infrared (NIR) digital orthophoto image acquired using a modified digital cameras mounted on an unmanned aerial vehicle (UAV) for aerial detection and monitoring of* Ganoderma *disease in oil palm. In this study, the orthophoto images were filtered using eight adaptive filters with filter sizes of 7x7 and 9x9. The filtered orthophoto images were then processed using three supervised image classifiers* i.e., *Maximum Likelihood (ML), Mahalanobis Distance (MD) and Neural Net (NN). The classifiers were used to categorise the* Ganoderma *disease severities into T0 (healthy), T1 (mild), T2 (moderate) and T3 (severe). The classification outputs were assessed using confusion matrix. The classification results suggested that RGB, NIR orthophoto only provided moderate classification accuracy of* Ganoderma *disease detection in oil palm. Future works should explore the utilisation of hyperspectral orthophoto images for detection of* Ganoderma *disease in oil palm.*

ABSTRAK

Penyakit Ganoderma *pada pokok sawit yang disebabkan oleh kulat* Ganoderma boninense *telah menyebabkan kehilangan signifikan pendapatan kepada Malaysia. Terdapat keperluan untuk membangunkan teknologi pengesanan penyakit* Ganoderma *berasaskan alat bawaan udara untuk mengurangkan masa dan kos, dan untuk meliputi kawasan ladang sawit yang luas. Kajian ini menganalisis kemampuan imej ortofoto digital merah-hijau-biru (RGB) dan inframerah hamper yang diambil menggunakan kamera digital yang telah diubah suai dan dipasang ke atas kenderaan udara tanpa pemandu (UAV) untuk pengesanan dan pemantauan melalui udara penyakit* Ganoderma *pada pokok sawit. Dalam kajian ini, imej ortofoto ditapis menggunakan lapan penapis boleh suai dengan saiz penapis 7x7 dan 9x9. Imej-imej yang telah ditapis kemudian diproses menggunakan tiga pengkelas imej berpenyelia iaitu pengkelas Kemungkinan Maksimum (ML), Jarak Mahalanobis (MD) dan Jaringan Neural (NN). Pengkelas-pengkelas tersebut digunakan untuk mengkategorikan keterukan penyakit* Ganoderma *kepada T0 (sihat), T1 (awal), T2 (sederhana) dan T3 (teruk). Hasil pengkelasan kemudian dinilai menggunakan matriks kekeliruan. Hasil pengkelasan menunjukkan bahawa ortofoto RGB dan NIR hanya memberikan ketepatan sederhana untuk pengesanan penyakit* Ganoderma *pada pokok sawit. Kajian masa hadapan perlu melihat kepada penggunaan ortofoto imej hiperspektral untuk pengesanan penyakit* Ganoderma *pada pokok sawit.*

Keywords: *Ganoderma*, red-green-blue, near infrared, orthophoto, UAV.

INTRODUCTION

Oil palm (*Elaeis guineensis* Jacq.) is recognised as one of the most important crops, with the highest oil yield compared to other cultivated oleaginous crops. The Malaysian palm oil obtained an export revenue of RM46.12 billion from India and the European Union markets (Kushairi *et al.*, 2018). The production of oil palm is susceptible to by *Ganoderma* disease, especially in Malaysia and Indonesia region. The *Ganoderma* disease caused by *Ganoderma boninense* fungus is the most destructive disease, causing major losses in the oil palm industry (Idris *et al.*, 2000; Roslan and Idris, 2012).

* Malaysian Palm Oil Board, 6, Persiaran Institusi, Bandar Baru Bangi, 43000 Kajang, Selangor, Malaysia. E-mail: mohamad.izzuddin@mpob.gov.my

\# Department of Geography, Faculty of Arts and Social Sciences, University of Malaya, 50603 Kuala Lumpur, Malaysia.

** Institute of Ocean and Earth Sciences, University of Malaya, 50603 Kuala Lumpur, Malaysia.

Ganoderma boninense is a fungus that is pathogenic to oil palm (Idris *et al.*, 2006; Rakib *et al.*, 2014). The fungus infects the roots of oil palm and moves into bole, usually only at the base of the oil palm (Rees *et al.*, 2009; Nuranis *et al.*, 2016). The infection leads to rotting at the palm base, thereby reducing the water and nutrient transport efficiency (Nur Sabrina *et al.*, 2012).

Recent advances in *Ganoderma* disease, several biocontrols and fungicides have been used to control and manage the disease (Idris *et al.*, 2006; Idris and Rafidah, 2008; Idris *et al.*, 2010a; Idris *et al.*, 2014) In addition, the *Ganoderma* disease in oil palm can also be detected, using several methods such as *Ganoderma* Selective Medium (GSM) (Ariffin *et al.*, 1993), Polyclonal Antibodies Enzyme-Linked Immunosorbent Assay (PAbs-ELISA) (Madihah *et al.*, 2014), Multiplex PCR-DNA Kit (Idris *et al.*, 2010a) and GanoSken Tomography (Mazliham *et al.*, 2006; Idris *et al.*, 2010b). However, these technologies have some limitations due to a lot of labour works, time-consuming and costly (Izzuddin, 2010).

The availability of low-cost light weight UAV equipped with modified consumer grade cameras that acquire RGB and NIR images has provided an opportunity for aerial perspective of vegetation and crop studies (Rasmussen *et al.*, 2016). Rasmussen *et al.*, 2016 showed that the vegetation indices (VI) from RGB and NIR images have an equal ability to quantify crop responses to several treatments. As it is carried out by ground-based recording using cameras and sensor, the bi-directional reflectance function (BRDF) effects must be considered to obtain good results. This gives an opportunity to study the capability of RGB and NIR images for detection of *Ganoderma* disease in oil palm.

Therefore, the objective of this study is to examine the capability of low-cost, light-weight UAV equipped with modified consumer grade digital camera of RGB and NIR for detection of *Ganoderma* disease in oil palm.

MATERIALS AND METHODS

Figure 1 shows the flow chart of methodology of this study.

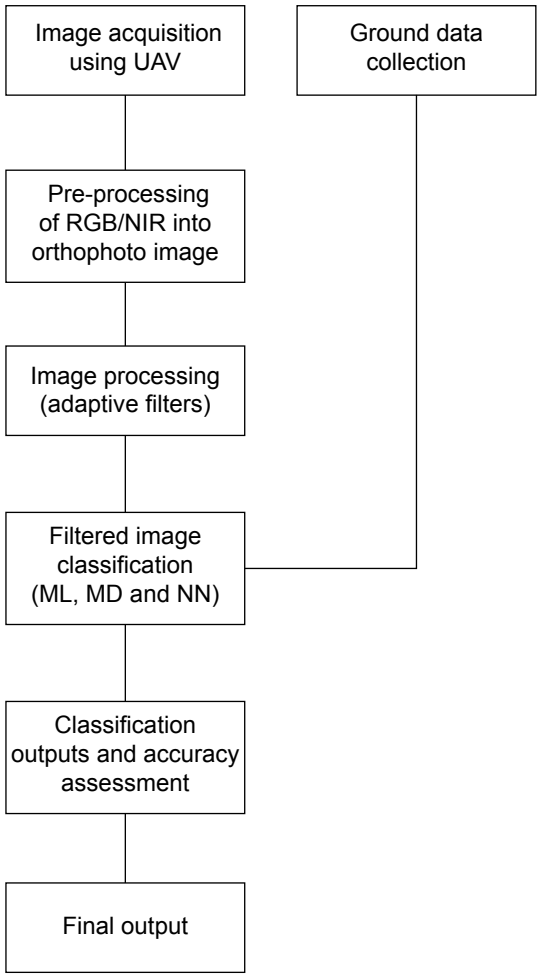

Figure 1. Flow chart of methodology.

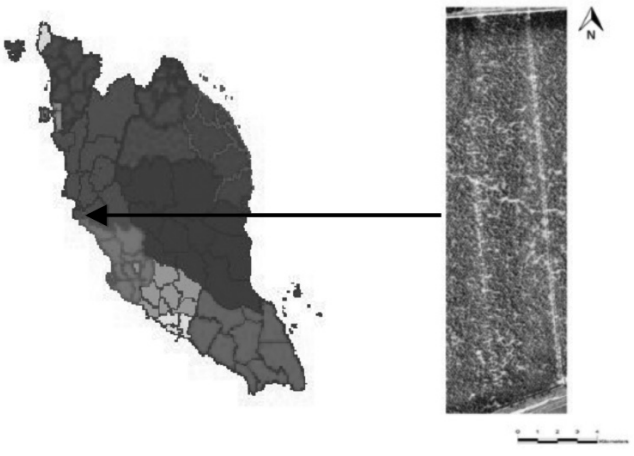

Figure 2. Location of the study area.

Study Area

The study was conducted in an oil palm plantation in Seberang Perak, Perak, Malaysia (*Figure 2*). The annual precipitation is 2256 mm and temperature is between 24°C and 34°C. The area consists of eight years old *Dura* x *Pisifera* (DxP) oil palms, covering an area of about 25 ha.

The study area was the first-generation of oil palm plantations that had previously been cleared from jungle area. The area topography was flat, undulating, with a good drainage system and adequate water supply, as the authorities have developed agricultural canals to assist other agricultural areas in the vicinity of the study area. The area has only reported the incidences of *Ganoderma* disease and no other pests, diseases, water stress and nutrient stress have been reported in the area.

Ground Data Collection

The data collected in the field consisted of *Ganoderma* disease census of each individual palm according to Disease Severity Index (DSI) of *Ganoderma* disease (*Table 1*) (Idris *et al.*, 2016) and coordinated sampling using Global Positioning System (GPS) image pre-processing.

UAV Data Acquisition

The data acquisition by UAV was conducted in June 2014 over the study area from 10 am to 12 pm under clear and sunny day with some cirrus cloud using Swinglet CAM UAV system (*Figure* 3), manufactured by Sensefly, a Parrot Company, Switzerland.

The UAV weighted around 0.5 kg included a camera with 80 cm wingspan, made of Expanded Polypropylene (EPP) foam, carbon structure and composite materials. The propulsion system consisted of an electric pusher propeller, a 100 Watt (W) brushless DC motor powered by a 11.1 V, 1350 mAh battery. For image acquisition, two modified Canon IXUS 220HS were used with the following specifications: 12.1 megapixels, 6.16 x 4.62 mm image sensor dimensions and 4000 x 3000 pixels as the maximum resolution. The UAV flight plan was setup using the ground control software (eMotion 2) while the software used for data processing was Postflight Terra LT.

One camera acquires digital images in red-green-blue (RGB) while the second camera acquires images in near-infrared (NIR) bands. The image acquisition settings were set to have 60% overlap between each image snapshot and 30% overlap between each flightpath. These were to generate a Digital Terrain Model (DTM) for producing an orthophoto mosaic of the RGB and NIR image. The spatial resolution of the RGB and NIR imageries was 10 cm GSD (ground sampling distance) with flight altitude of 150 m above the ground. The UAV maximum flight time was 30 min with a normal cruise speed of about 36 km hr^{-1} during image acquisition.

Figure 3. Swinglet with modified Canon IXUS 220HS.

Image Pre-processing

A total of 98 snapshots of the raw digital images for each RGB and NIR were acquired over the study plot. The images were tagged with ground coordinates and data from the Inertial Measurement Unit (IMU) system that were important to generate an orthophoto image mosaic of the study area.

The pre-processing was conducted using the Postflight Terra LT software. The raw images were georeferenced to the Universal Transverse Mercator (UTM) under World Geodetic Survey 1984 (WGS-84) coordinate system using a set of Ground Control Points (GCPs) at the fields measured with Differential Global Positioning System (DGPS). A DTM was generated for orthorectification and the resulted orthophoto images of RGB and NIR were shown in *Figures 4a* and *4b*.

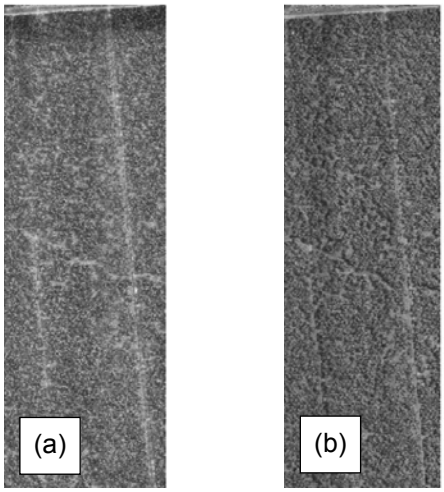

Figure 4. (a) Digital orthophoto mosaic image of RGB; (b) Digital orthophoto mosaic image of NIR.

Image Processing

The image processing involved several steps: 1) applying adaptive filters with different kernel window sizes, 2) supervised classification and 3) accuracy assessment. In this study, two filters with window sizes of 7x7 and 9x9 were selected for the adaptive filters. Eight adaptive filters were used in this study: 1) Lee; 2) Enhanced Lee; 3) Frost; 4) Enhanced Frost; 5) Gamma; 6) Kuan; 7) Local Sigma; and 8) Bit Error. The adaptive filters used the standard deviation of image pixels within a local box circling each pixel to calculate a new pixel value. It reduced the complexity of spectral signatures from each individual oil palm canopy.

The Lee filters were used to smooth noisy and speckled image with additive or multiplicative intensity component. The Enhanced Lee conserved

the texture of the objects and used local statistics such as variations and coefficients within each filter window. Each pixel was categorised into homogeneous, heterogeneous and point target (Lopes *et al.*, 1990).

The Frost filter converted the pixels of the filtered image with a value calculated based on the distance from the filter centre, the damping factor, and the local variance (Shi and Fung, 1994). Meanwhile, the Enhanced Frost filter adapted Frost filter and similarly used local statistics (coefficient of variation) within individual filter window (Lopes *et al.*, 1990). In Gamma filter, the gamma coefficients were distributed and the multiplicative noise model was transferred into an additive noise model.

The Local Sigma preserved the fine image detail and greatly reduced speckle. The Local Sigma filter used the local standard deviation computed from the filter box to determine the valid pixels within the filter window (Eliason and McEwen, 1990). Bit Error filters were used to remove bit-error noise that were caused by image spikes from isolated pixels of extreme values unrelated to the image scene (Eliason and McEwen, 1990).

Then, the orthophoto images of both RGB and NIR were classified using supervised classifiers according to the *Ganoderma* disease categories (*Table 1)*. Three supervised image classifiers were used in this study which are 1) Maximum Likelihood (ML); 2) Mahalanobis Distance (MD) and 3) Neural Net (NN). The ML is a parametric classifier that classifies unknown pixels based on the probability threshold and each pixel is allocated to the class with the maximum probability (Shojanoori *et al.*, 2016).

TABLE 1. *Ganoderma* DISEASE SEVERITY INDEX (DSI) AND DESCRIPTION

DSI	Category	Visual symptoms
T0	Healthy	Canopy looks healthy, no presence of *Ganoderma* white mycelium, small white button or fruiting bodies.
T1	Mild infection	Canopy looks healthy, but presence of *Ganoderma* white mycelium, small white button, fruiting bodies or rotting at the palm base.
T2	Moderate infection	Canopy yellowing and wilting (<30%), presence of fruiting bodies and rotting at the palm base.
T3	Severe infection	Canopy yellowing and wilting (>30%), presence of fruiting bodies and rotting at the palm base.

Meanwhile, MD is similar to ML classification by undertaking all class covariances are equal and assuming the histograms of the image bands have normal distributions (Canty, 2014). Furthermore, NN is an advanced image classification technique that uses standard back propagation for supervised learning, which consists of one input layer, at least one hidden layer and one output layer. The algorithm adjusted the weights in the node during learning processes to minimise the difference between the output node activation and the output (Perumal and Bhaskaran, 2010).

In this study, the image properties of each DSI were extracted from the orthophoto image using Region of Interest (ROI) tool in ENVI 5.0 software. The ROI selection was conducted to extract Digital Numbers (DN) that represents the *Ganoderma* DSI and also non-oil palm features in the image as training samples. Thirty ROI samples for each DSI were collected as training samples and 10 ROI samples as classifier testing samples. The testing samples are important to assess the accuracy of the classification outputs produced by each image classifiers used. The assessment of accuracy was conducted using the confusion matrix and Kappa coefficient statistic.

Confusion matrix is also known as error matrix (Kohavi and Provost 1998). Confusion matrix is associated with the method, which assess the capability of classifier for displaying the predicted and actual classification of features in image, thus summarising the relationship between the two sources of information (Jensen, 2005). The confusion matrix qualitatively measured the accuracy of the classification (0-100%). The percentage of accuracy can also be related to the Kappa coefficient. A good percentage of accuracy must exceed 80% (Viera and Garret 2005).

RESULTS

Image Filtering and Classification

The image filtering and classification were conducted using ENVI 5.0 software. The filtered orthophoto image was then classified into *Ganoderma* DSI. The classification processes were conducted using the ML, MD and NN techniques. For each RGB and NIR image, the classification outputs were in pseudo-colour images that represented the individual oil palm categories corresponding to their *Ganoderma* DSI.

Tables 2 and *3* lists the outputs of the classification and their accuracies.

TABLE 2. SUPERVISED CLASSIFICATION USING 7x7 FILTER SIZE ON RGB IMAGE

Filter kernel size	**Frost**	**RGB Gamma 7 x 7**	**Gamma**	**Enhanced Frost**	**RGB Enhanced Lee 9 x 9**	**Local Sigma**
Classification output	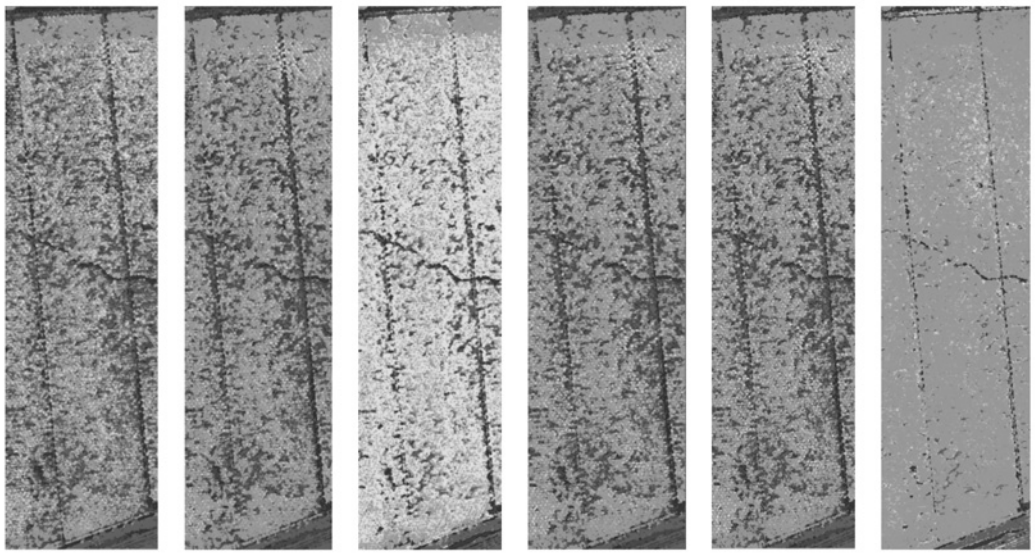					
Classifier	ML (a)	MD (b)	NN (c)	ML (d)	MD (e)	NN (f)
Overall accuracy (%)	33.7	34.2	34.4	34.5	34.5	37.6
Kappa coefficient	0.1954	0.1981	0.2027	0.2013	0.2016	0.2090

Note: (a) ML - Frost (c) NN - Gamma (e) MD - Enhanced Lee
(b) MD - Gamma (d) ML - Enhanced Frost (f) NN - Local Sigma

DISCUSSION

The results tabulated in *Tables 2* and *3* showed that the Enhanced Frost filter had the highest accuracy followed by Frost, Enhanced Lee, Lee, Local Sigma, Gamma and Bit Error. Meanwhile, the Kuan filter was considered to be detrimental to the analysis. When the image was classified using ML and NN classifier, the Local Sigma gave higher accuracy than other filters, followed by Enhanced Frost and Enhanced Lee. The results also demonstrated that MD produced lower accuracy compared to ML and NN classifiers.

The suitable filters for RGB orthophoto image were Frost, Gamma, Enhanced Frost, Enhanced Lee and Local Sigma. The RGB orthophoto image using NN classification and filtered by Local Sigma (with 9x9 filter size) showed the highest accuracy (37.6%) compared to others. The range of accuracy for analysis of RGB orthophoto image is considered low, from 33.7% to 37.6% only. On the other hand, the NIR orthophoto image analysis provided better classification accuracy than RGB orthophoto, ranging from 34.8% to 41.4%. However, it was still categorised as low overall accuracy for the detection of *Ganoderma* disease in oil palm. The results are consistent with Minarik and Langhammer (2016) that used multispectral UAV photogrammetry for detection and tracking of forest disturbance dynamics. Their results suggested that the RGB and NIR images from UAV had low to moderate capability to discriminate and identify forest disturbances dynamics. Other than that, a study conducted by Lehmann *et al.* (2015) on coloured infrared images over forest area to monitor pest infestation levels also showed moderate classification accuracy with Kappa coefficient of 0.67 and 0.66. They believe that the study failed to achieve good classification accuracy due to the sun-illumination effects, the shape of leaves and branches, and lack of albedo characteristic information. Other than that, Garcia-Ruiz *et al.*, 2013 used six spectral bands camera mounted on UAV to detect Huanglongbing in orange trees and proposed moderate results (28%-45% and 61%-74%) for certain study areas.

These results indicated that the classification of homogeneous crops using RGB and NIR orthophoto images recorded in the Digital Number (DN) properties usually give low to moderate accuracy. Further study on detection of *Ganoderma* disease in oil palm has to be performed on the RGB and NIR images that are measured in percentage

TABLE 3. SUPERVISED CLASSIFICATION USING 7x7 FILTER SIZE ON NIR IMAGE

Filter kernel size	NIR Enhanced frost	NIR Lee 7 x 7	Lee	Enhanced Lee	NIR Lee 9 x 9	Local Sigma
Classification output	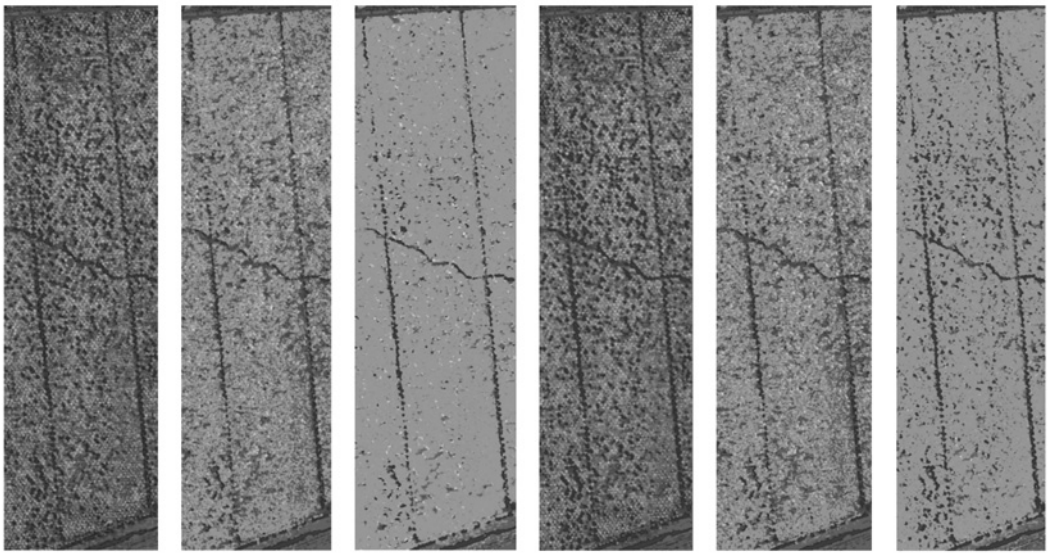					
Classifier	ML (a)	MD (b)	NN (c)	ML (d)	MD (e)	NN (f)
Overall accuracy (%)	41.2	34.8	41.3	40.9	34.8	41.4
Kappa coefficient	0.2532	0.2140	0.2824	0.2515	0.2135	0.2836

Note: (a) Ml - Enhanced Frost (c) Nn - Lee (e) Md - Lee
(b) Md - Lee (d) Ml - Enhanced Lee (f) Nn - Local Sigma

of reflectance and hyperspectral UAV system for better recorded spectral response from the crops compared to DN only.

CONCLUSION

In this study, the performance of ML, MD and NN classifiers for *Ganoderma* DSI classification was compared. The results showed that the NN classifier had better performance than others. However, the RGB and NIR image recorded in DN properties could only provide low to moderate classification accuracy for *Ganoderma* DSI in oil palm. Further works can be conducted on multispectral and hyperspectral UAV system which were examined through spectral reflectance properties rather than solely DN.

ACKNOWLEDGEMENT

The authors would like to acknowledge the University of Malaya Research Grant (UMRG) (RP023-2012E) for funding this study and Postgraduate Research Grant (PPP) (PG273-2015B). The authors also thank *Ganoderma* and Disease Research of Oil Palm Unit (GanoDROP), Malaysian Palm Oil Board (MPOB) for providing technical and expertise assistance.

REFERENCES

Ariffin, D; Idris, A S and Khairuddin, H (1993). Confirmation of *Ganoderma* infected palm by drilling technique. *Proc. of the 1993 PORIM International Palm Oil Congress: Update and Vision (Agriculture)*. PORIM, Bangi. p. 735-738.

Canty, M J (2014). *Image Analysis, Classification and Change Detection in Remote Sensing: With Algorithms for ENVI/IDL and Phyton*, Third Edition. CRC Press, 2014.

Eliason, E M and A S McEwen, (1990). Adaptive Box Filters for Removal of Random Noise from Digital Images. *Photogrammetric Engineering & Remote Sensing, 56(4)*: 453-458

Garcia-Ruiz, F; Sankaran, S; Maja, J M J and Lee, W S (2013). Comparison of two aerial imaging platforms for identification of huanglongbing-infected citrus trees. *Computers and Electronics in Agriculture, 91*: 106-115.

Idris, A S; Ariffin, D; Swinburne, T R and Watt, T A (2000). The identity of *Ganoderma* species responsible for BSR disease of oil palm in Malaysia - pathogenicity test. *MPOB Information Series 77b*: 1-4.

Idris, A S; Kushairi, D; Ariffin, D and Basri, M W (2006). Technique for Inoculation of oil palm germinated seeds with *Ganoderma*. *MPOB Information Series No. 314*: 1-4.

Idris, A S and Rafidah, R (2008). Enzyme linked immunosorbent assay-polyclonal antibody (elisa-pab). *MPOB Information Series No. 430*: 1-4.

Idris, A S; Rajinder, S; Madihah, A Z and Wahid, M B (2010a). Multiplex PCR-DNA kit for early detection and identification of *Ganoderma* species in oil palm. *MPOB Information Series* 531: 1-4.

Idris, A S; Mazliham, M S; Loonis, P and Wahid, M B (2010b). GanoSken for early detection of *Ganoderma*. *MPOB Information Series No. 499*: 1-4.

Idris, A S; Nur Rashyeda, R and Madihah, A Z (2014). Kawalan *Ganoderma* sawit menggunakan teknologi. *Prosiding Persidangan Pekebun Kecil Sawit Kebangsaan* 2014, Sarawak, August 11-12: 70- 85.

Idris, A S; Nur Rashyeda, R; Mohd Hefni, R; Shamala, S and Norman, K (2016). *Standard Operating Procedures (SOP) Guidelines for Managing* Ganoderma *Disease in Oil Palm*. MPOB, Bangi.

Izzuddin, M A (2010) *Early Detection of* Ganoderma *Disease in Oil Palm (Elaeis guineensis Jacq.) using Field Spectroscopy*. Master Thesis. Universiti Putra Malaysia. p. 1-219.

Jensen, J R (2005). Introductory Digital Image Processing: A Remote Sensing Perspective, 2nd ed., Prentice Hall Series in Geographic Information Science, (Upper Saddle River: New Jersey).

Kohavi, R and Provost, F (1998). *Glossary of Terms Special Issue on Applications of Machine Learning and the Knowledge Discovery Process. Machine Learning,* 30(2/3),271--274. Retrieved from http://robotics.stanford.edu/~ronnyk/glossary.html

Kushairi, A; Loh, S K; Azman, I; Hishamuddin, E; Meilina-Ong, A; Izuddin, Z B M N; Razmah, G; Shamala, S and Parveez, G K A (2018). Oil palm economic performance in Malaysia and R&D progress in 2017. *J. Oil Palm Res., 30(2)*: 163-195.

Lehmann, J; Karl, R; Nieberding, F; Prinz, T and Knoth, C (2015). Analysis of unmanned aerial system-based CIR images in forestry - A new perspective to monitor pest infestation levels. *Forests, 6*: 594-612. DOI:10.3390/f6030594.

Lopes, A; Touzi, R and Nezry, E (1990). Adaptive speckle filters and scene heterogeneity. *IEEE Transactions on Geoscience and Remote Sensing*, *28*: 992-1000.

Madihah, A Z; Idris, A S and Rafidah, A R (2014). Polyclonal antibodies of *Ganoderma boninense* isolated from Malaysia oil palm for detection of basal stem rot disease. *African J. Agri. Res., 13*: 3455-3463. DOI:10.5897/A.

Mazliham, M S; Pierre, L and Idris, A S (2006). Mass function initialization rules for *Ganoderma* infection detection by tomography sensor. *Proc. of the 2nd IASTED International Conference on Computational Intelligence, CI 2006*. p. 377-386.

Minarik, R and Langhammer, J (2016). Use of a Multispectral UAV Photogrammetry for Detection and Tracking of Forest Disturbance Dynamics. The International Archives of the Photogrammetry, Remote Sensing and Spatial Information Sciences, XXIII ISPRS Congress, 12-19 July 2016, Prague, Czech Republic. p. 711-718.

Nuranis, I; Kamaruzaman, S; Khairulmazmi, A; Mohd Shukri, I; Zulkifli, H and Idris, A S (2016). Leaf nutrient status in relation to severity of *Ganoderma* infection in oil palm seedlings artificially infected with *Ganoderma boninense* using root inoculation technique. *Oil Palm Bulletin*, *72*: 25-31.

Nur Sabrina, A A; Sariah, M and Zaharah, A R (2012). Suppression of basal stem rot disease progress in oil palm (*Elaeis guineensis*) after copper and calcium supplementation. *Pertanika J. Trop. Agric. Sci. 35*: 13-24.

Perumal, K and Bhaskaran, R (2010). Supervised classification performance of multispectral images. *J. Computing*, 2: 124-129.

Rakib, M R M; Bong, C F J; Khairulmazmi, A and Idris, A S (2014). Genetic and morphological diversity of *Ganoderma* species isolated from infected oil palms (*Elaeis guineensis*). *Int. J. Agriculture and Biology, 16*: 691-699.

Rasmussen, J; Georgios N; Nielsen, J; Svensgaard, J; Poulsen, R N and Christensen, S (2016). Are vegetation indices derived from consumer-grade cameras mounted on uavs sufficiently reliable for assessing experimental plots? *European J. Agronomy 74*: 75-92. DOI:10.1016/j.eja.2015.11.026.

Rees, R W; Flood, J; Hasan, Y; Potter, U and Cooper, R M (2009). Basal stem rot of oil palm (*Elaeis guineensis*) mode of root infection and lower stem invasion by *Ganoderma boninense. Plant Pathology, 58*: 982-989. DOI:10.1111/j.1365-3059.2009.02100.x.

Roslan, A and Idris, A S (2012). Economic impact of *Ganoderma* incidence on Malaysian oil palm plantation – A case study in Johor. *Oil Palm Industry Economic J., 12*: 24-30.

Shojanoori, R; Shafri, H Z M; Mansor, S and Ismail, M H (2016). The use of World-View-2 satellite data in urban tree species mapping by object-based image analysis technique. *Sains Malaysiana*, *45*: 1025-1034.

Shi, Z and Fung, K B (1994). A comparison of digital speckle filters. *Proc. of IGARSS, 94*. p. 2129-2133.

Viera, A J and Garrett, J M (2005). Understanding interobserver agreement: The kappa statistic. *Family Medicine*, *37*: 360-363.